SIMULATION OF PHYSICAL PROCESSES

DOI: 10.18721/JPM.11405
УДК 532.5.013.13

THE STRUCTURE OF A NATURAL CONVECTIVE FLOW OVER A HORIZONTAL HEATED DISC AT SMALL GRASHOF NUMBERS

E.F. Khrapunov, Yu.S. Chumakov

Peter the Great St. Petersburg Polytechnic University, St. Petersburg, Russian Federation

In the paper, the results of physical and numerical simulation of a natural convective flow formed over a heated horizontal disk with small Grashof numbers have been presented. The characteristics of the near-wall flow region and of the ascending flow one were considered in detail. On the basis of experimental and calculated data, the geometric flow characteristics, namely temperature and dynamic thicknesses, were determined. A good agreement between the experimental results and numerical simulation data was achieved. The results obtained were also compared with published data. The distribution of the vertical velocity component in the near-wall layer was determined. The analysis of the basic characteristics of heat exchange, namely the local and integral Nusselt numbers, was carried out.

Keywords: natural convection, natural convective plume, flow structure, physical experiment, numerical simulation

Citation: E.F. Khrapunov, Yu.S. Chumakov, The structure of a natural convective flow over a horizontal heated disc at small Grashof numbers, St. Petersburg Polytechnical State University Journal. Physics and Mathematics. 11 (4) (2018) 44–56. DOI: 10.18721/JPM.11405

СТРУКТУРА СВОБОДНОКОНВЕКТИВНОГО ТЕЧЕНИЯ НАД ГОРИЗОНТАЛЬНЫМ НАГРЕТЫМ ДИСКОМ ПРИ НЕБОЛЬШИХ ЧИСЛАХ ГРАСГОФА

Е.Ф. Храпунов, Ю.С. Чумаков

Санкт-Петербургский политехнический университет Петра Великого,
Санкт-Петербург, Российская Федерация

В статье представлены результаты физического и численного моделирования свободноконвективного потока, формирующегося над нагретым горизонтальным диском при небольших числах Грасгофа. Подробно рассмотрены характеристики области пристенного течения и области восходящего потока. На основании экспериментальных и расчетных данных определены геометрические характеристики потока – температурные и динамические величины толщины. Получено хорошее соответствие между результатами физического эксперимента и численного моделирования. Кроме того, проведено сравнение с опубликованными литературными данными. Получено распределение вертикальной компоненты скорости в пристенном слое. Проанализированы основные характеристики теплообмена – локального и интегрального чисел Нусельта.

Ключевые слова: свободная конвекция, свободноконвективный факел, структура потока, физический эксперимент, численное моделирование

Ссылка при цитировании: Храпунов Е.Ф., Чумаков Ю.С. Структура свободноконвективного течения над горизонтальным нагретым диском при небольших числах Грасгофа // Научно-технические ведомости СПбГПУ. Физико-математические науки. 2018. Т. 11. № 4. С. 47–60. DOI: 10.18721/JPM.11405

Introduction

Major advances in the field of natural convective heat transfer have been made in studies of currents along a vertical surface, i.e., with the gravitational acceleration vector parallel to the main direction of the fluid flow. These advances have been made possible by progress in developing the theory of forced convective boundary layer. Natural convection evolves because of surface heating, and, as a consequence, a natural convective boundary layer forms on a sufficiently long vertical surface. The basic patterns in the behavior of such a layer are very similar to those of a forced convective boundary layer which has already been well-studied. In particular, similar to forced convection, regions of laminar, transient, and turbulent flow exist in a natural convective boundary layer.

The situation is different if the heated surface is horizontal or heavily inclined with respect to the gravitational acceleration vector. Natural convection heat transfer in fluid observed on such surfaces has a complex character, due to interaction of separated ascending flow over its surface and the surface layer induced by a favorable pressure drop that is in turn generated by this flow.

Analysis of such interaction is fairly complicated, which is why various simplified models of heat transfer have been proposed in literature. For example, two extreme cases are considered in [1, 2]:

in the first case, the heated surface is so small that it can be replaced by a point heat source with an axisymmetric natural convective ascending plume forming above it;

in the second case, the surface is so large that the contribution from the central part of the surface with the ascending plume to heat transfer can be neglected in the limit. The ascending plume only indirectly affects heat transfer from the surface, forming only near-surface flow due to the ejecting effect of this plume.

Thus, determining the intensity of heat transfer from the surface is reduced to solving the problem on flow over a heated semi-infinite plate. For example, two-dimensional equations of the near-surface boundary layer were solved in some approximation in a number of studies [3–5]; as a result, practically important formulae for calculating the intensity of heat transfer from a heated horizontal surface were obtained (summary table for the dependences is given in [6]).

Let us consider the first extreme case when an ascending plume is formed above a point heat source. In this case, surface does not directly affect the flow; only heat transfer of this surface is taken into account in order to set the intensity of the point heat source. Solving problems in a statement equivalent to this one allowed to obtain analytical and numerical solutions in the self-similar approximation. In particular, the influence of the strength of the heat source on various characteristics of the plume was established; for example, it was confirmed that the decrease in temperature along the height followed a power law, while the width of the ascending plume varied as the Grashof number to the power of 1/4 (the Grashof number is the governing parameter of the problem).

Evidently, two extreme case are insufficient for describing the diverse range of problems on natural convection heat exchange in fluid flowing from a heated horizontal surface. The case when the surface cannot be replaced by a point heat source of heat but also is not so large as to consider it semi-infinite and to neglect the influence of the ascending plume on heat exchange is of the greatest interest from a practical standpoint. In other words, not only the influence of the ascending plume at the center of the disk, but also of the near-surface flow along its surface has to be included in the calculations.

We should note that the near-surface layer develops in spite of the action of the Archimedes (buoyant) force, which directed not along the flow but perpendicular to it, i.e., the motion is due to indirect causes. In [6], the flow was generated by a negative pressure gradient induced by a plume ascending from the center of the disk [6].

In this study, we have experimentally and numerically analyzed the influence of the heating intensity of a horizontal disk on heat transfer and on the structure of the flow above the disk for small Grashof numbers.

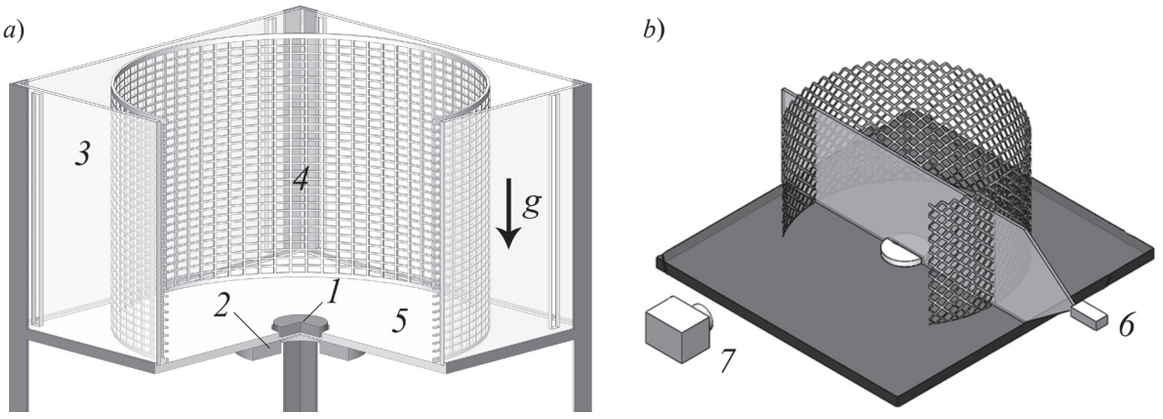

Fig. 1. Schematics for experimental testbed (*a*) and visualization of the structure of natural convective flow (*b*)
heated disk *1*, heat exchanger element *2*, permeable chamber walls *3*, protective grid *4*, horizontal plate *5*, laser and optical system *6*, photocamera *7*; *g* is the vector of gravitational acceleration

Analysis of the results of numerical simulation was largely based on experimental data, in particular, on visualizations of air flow over a heated disk, presented earlier in [7].

Experimental testbed and experimental methods

A schematic view of the experimental testbed is given in Fig. 1. The main element of the testbed is a heated brass disk *1* with a diameter of 190 mm and a thickness of 8 mm. Its bottom is in contact with heater *2*. A special paste with high thermal conductivity is used to improve the thermal contact; a thermocouple junction (not shown in the figure) is placed into a layer of this paste to control the temperature of the bottom of the disk. The temperature of the disk is maintained by a controller (not shown in the figure), which turns on/off the heater depending on whether the temperature set corresponds to the temperature detected by the thermocouple.

Thus, conditions close to constant temperature are imposed on the bottom of the disk, while the temperature on top of the disk is determined by conjugate heat exchange with air.

The base of the protective chamber (see Fig. 1) is a horizontal plate *5* with a round central cutout; disk *1* with a gap of *5* mm is inserted into the cutout. The top of the disk protrudes over the upper surface of the plate by 6 mm. The shell of heat exchanger *2*, fitting tightly against the lower surface of horizontal plate *5* and maintaining its constant temperature at 16–18°C, covers the gap from below.

The testbed is equipped with a coordinate system (not shown in the figure) allowing to move a probe (for example, a temperature sensor) above the disk by using programatically controlled stepper motors. The accuracy of movement is 0.50 mm in the horizontal and 0.05 mm in the vertical plane.

Particular care was taken to measure the temperature of the air over the heated disk. A tungsten wire sensor with a diameter of 5 μm and a length of 2 mm was used to obtain the instantaneous temperature value. Due to its small size, the sensor has an almost instant response to sudden changes in temperature, considerably expanding (together with the corresponding electronic equipment) the frequency range of measurements. The procedure of measuring the temperature at a selected point in space above the disk consisted in converting a continuous analog signal over a certain period of time depending on the number of samples with a given frequency (3000 samples with a sampling frequency of 50 Hz) to digital form. The digital image obtained this way for the variation of instantaneous temperature with time at a given point in space was practically undistorted. The mean temperature and intensity of instantaneous temperature fluctuations were calculated by initial processing of digitized signal. In addition, the recorded instantaneous temperature was saved for further correlational and spectral analysis.

In addition to point temperature measurements, numerous photos and videos of the flow under consideration were taken to gain a more complete picture of the structure of natural convective flow forming over the heated disk. The

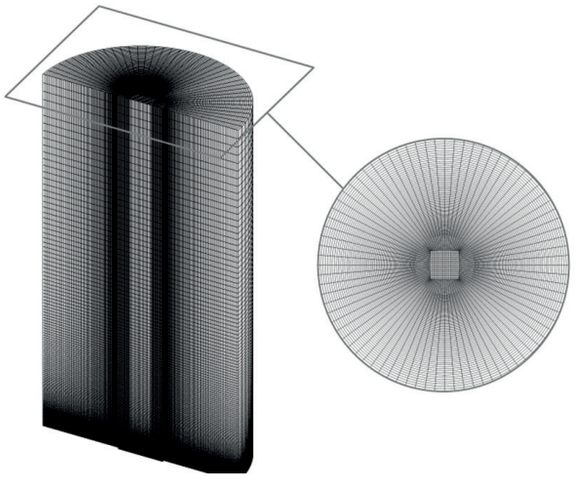

Fig. 2. Example of a computational grid in the solution domain of the equations

flow was visualized by the scheme shown in Fig. 1, *b*. The volume where the flow formed was seeded in advance with smoke particles that were then carried by the flow and, accordingly, visualized it.

The laser sheet technique was used for detailed analysis of the flow structure and for considering individual fragments of the flow. In our case, a laser whose beam was reshaped into a plane using an appropriate optical system was used as a light source. Fragments of smoke entering the plane of the sheet were brightly illuminated by it, visualizing a selected fragment of the flow that was recorded by photo or video camera.

Numerical model

The ANSYS Fluent code allowing to solve the Navier–Stokes equations in the Boussinesq approximation for a compressible medium was used for numerical simulation. Based on experimental data, we assumed that the flow was laminar in the selected range of Grashof numbers

$$Gr = (0.89 - 9.50)\cdot 10^6$$

for three-dimensional flow with conjugate heat exchange between the heated disk and the ambient environment.

A fragment of the computational domain with a grid covering it is shown in Fig. 2. The dimensions of the computational domain exactly match those of the experimental test-bed. A quasi-structured grid including 1 million elements was used, with the grid lines clustered to the expected boundaries of the plume and to the lower surface of the computational domain.

The parameters of air and brass used in numerical simulation are given in Table.

It follows from the data in Table that the air parameters used in the simulation were assumed to be constant, since they do not vary substantially in the given temperature range.

The boundary conditions were imposed as follows in the calculations. The temperature of the lower surface of the disk was set and remained constant during the calculation, the temperature of the horizontal surface of the computational domain was also considered constant and equal to the temperature of the ambient air (293 K). The temperature of the upper surface of the disk was determined from the condition of conjugate heat exchange with air adjacent to the surface. Conditions of zero gauge pressure were set for all other boundaries (lateral and upper). The following constraints

Table

Parameter values used in numerical simulation

Object	Parameter	Notation	Unit	Value
Air	Specific heat capacity	c_p	J/(kg·K)	1006.43
	Thermal conductivity	λ	W/(m·K)	0.0242
	Coefficient of thermal expansion	β	K^{-1}	0.00366
	Kinematic viscosity	υ	m^2/s	$1.8\cdot 10^{-5}$
Brass	Density	ρ^{br}	kg/m^3	8500
	Specific heat capacity	c_p^{br}	J/(kg·K)	380
	Thermal conductivity	λ^{br}	W/(m·K)	130

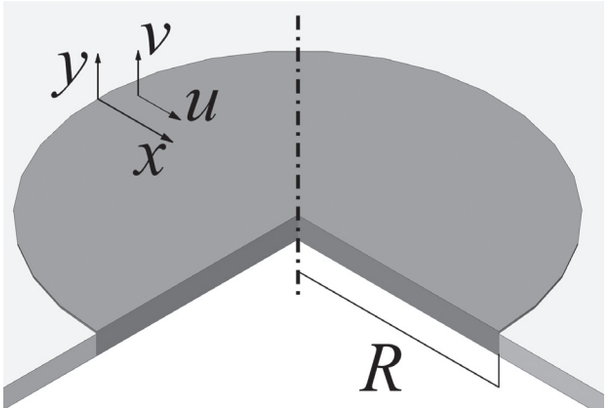

Fig. 3. Coordinate system x, y related to the surface of a disk of radius R;
u, v are the components of the air flow velocity.

were imposed on the air flowing into the computational domain through these boundaries: that the air temperature remained constant (293 K), and that the vector of its propagation velocity was always perpendicular to the corresponding inflow boundary.

The coordinate system was chosen so that the radial (or longitudinal) coordinate x started from the edge of the disk and was directed toward its center, and the axial coordinate y was directed upward, perpendicular to the surface of the disk. Accordingly, we denoted the longitudinal component of the velocity by u, and the axial component by v (Fig. 3).

We introduced dimensionless variables, using the ratio υ/R as the velocity scale (the kinematic viscosity υ to the radius R of the disk):

$$x^* = x/R,\ y^* = y/R;$$

$$u^* = u \cdot R/\upsilon,\ v^* = v^* = v \cdot R/\upsilon;$$

$$\theta = (T - T_a)/(T_w - T_a),$$

where T_w, T_s are the temperatures of the upper surface of the disk and the air at the outer boundary of the computational domain, respectively.

A constant temperature T_c was set on the lower surface of the disk as a boundary condition. In this study we have carried out numerical simulation for temperatures equal to 303, 313, 333 and 353 K.

Simulation results and analysis

As noted above, the flow generated over the heated disk can be divided into two regions: the near-surface layer and the ascending plume. Let us first analyze the experimental and numerical data obtained for the flow in the near-surface layer.

Fig. 4, *a* shows the profiles of dimensionless temperature θ, and Fig. 4, *b* the profiles of dimensionless longitudinal velocity u^* normal to the disk surface at different values of the dimensionless longitudinal coordinate x^* for the Grashof number $\mathrm{Gr} = 3.5 \cdot 10^6$. The Grashof number is defined as follows from now on:

$$\mathrm{Gr} = \frac{g\beta\left(T_0 - T_a\right)R^3}{\upsilon^2}, \qquad (1)$$

where T_0 is the temperature of the lower surface of the disk, controlled in the experiment and set as the boundary condition in numerical simulation, g is the gravitational acceleration, β is the coefficient of thermal expansion.

Temperature profiles exhibit a sharp transition from surface temperature to ambient air temperature over the greatest part of the disk. The temperature layer apparently thickens upon approaching the vertical axis of the disk. The change in longitudinal velocity along the height is not monotonic; a local maximum appears, whose vertical coordinate increases approaching the center of the disk. In addition, the maximum velocity also increases from the edge to the center of the disk, approximately up to the coordinate $x^* = 0.6$ and then decreases down to zero, which indicates that longitudinal near-surface flow is transformed into vertical ascending flow.

The axial component of the velocity vector has a considerable effect on the formation of the flow structure near the disk. Notably, we could find virtually no data in literature regarding the distribution of this component in the near-surface layer. Nevertheless, a change in axial velocity in the near-surface region can be of considerable interest for determining the characteristics of the near-surface layer, as well as for understanding the deformation this layer undergoes as it evolves. Fig. 4, *c* shows the axial velocity profiles along the normal to the disk surface for different values of the x^* coordinate. Pronounced local maxima are observed on the profiles, with the sign of the maximum value changing along the axial coordinate x^* from the edge of the disk to its center. In particular,

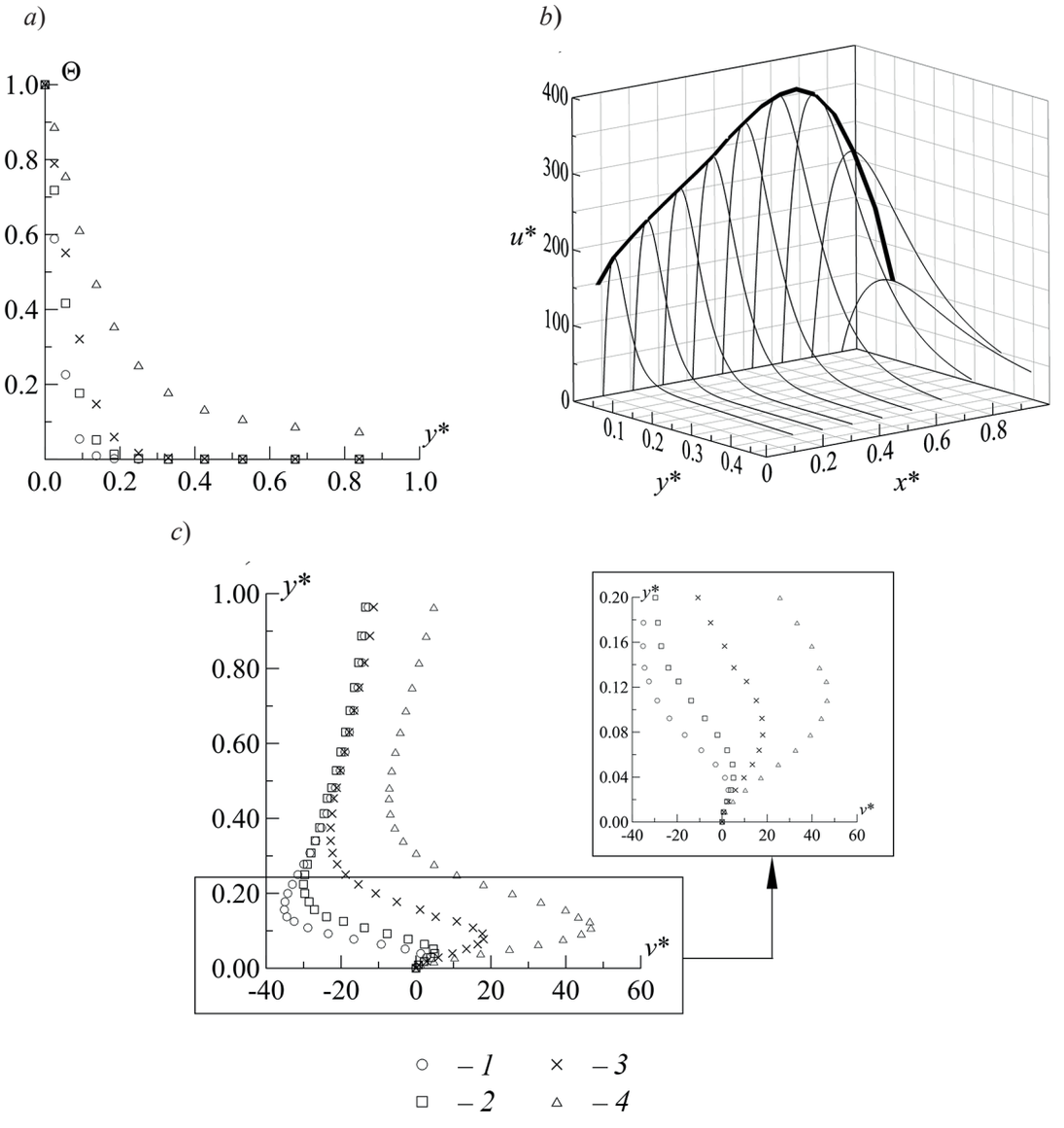

Fig. 4. Experimental (*a*) and calculated (*b*, *c*) profiles of dimensionless quantities, obtained by simulation of the flow in the near-surface layer: temperatures across this layer (*a*), longitudinal velocity inside the layer (*b*) and axial velocity across the layer (*c*) for different values of the dimensionless longitudinal coordinate x^* with the Grashof number $Gr = 3.5 \cdot 10^6$. Values of x^*: 0.16 (*1*), 0.37 (*2*), 0.58 (*3*), 0.79 (*4*)

not only the maximum value but also the axial velocity at a large distance from the disk surface turn out to be negative in the interval $0 \le x^* \le 0.4$. Similar behavior is characteristic for the longitudinal velocity profile with $x^* \ge 0.8$ but the difference is that the sign of velocity remains positive. With $x^* = 0.58$ the velocity profile undergoes sign alternation: the velocity is positive near the surface and negative above it. This behavior of axial velocity, together with the longitudinal component, determines the resulting orientation of the velocity vector. Due to this orientation, the effect of the buoyant (Archimedes) force becomes noticeable at a distance of the order of $(0.7-0.8)R$ from the edge of the disk, and the buoyant force becomes the main factor governing the evolution of the flow approaching the center of the disk (or the plume axis), i.e., an ascending plume is formed.

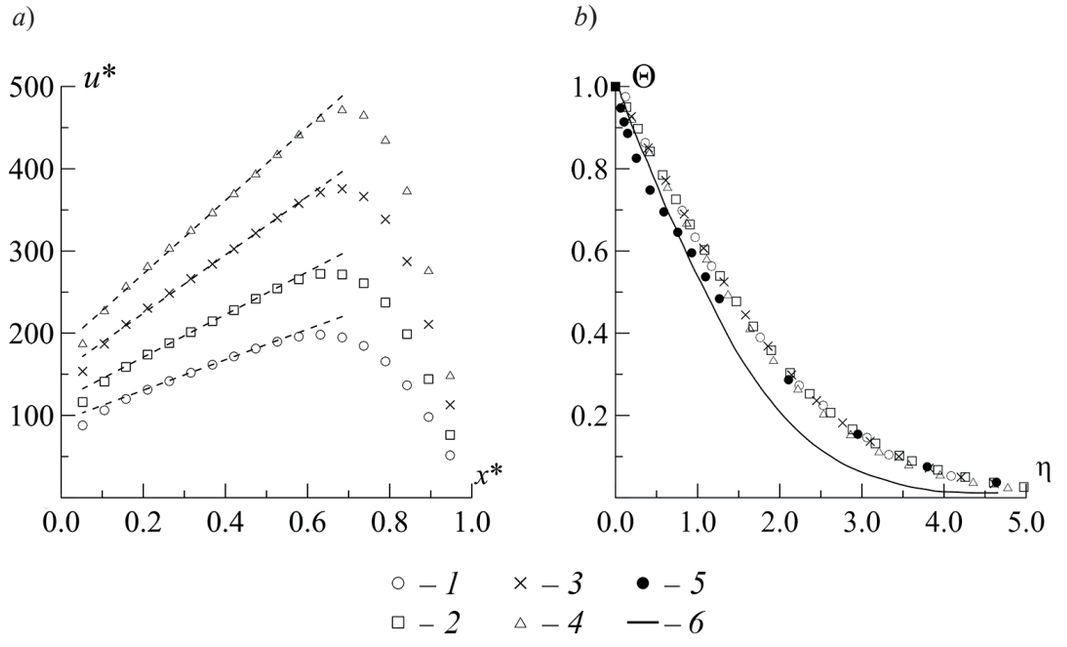

Fig. 5. Calculated (*1*–*4*, data from [5] for comparison (*6*)) and experimental (*5*) distributions of dimensionless quantities in the near-wall layer:
maximum radial velocity inside this layer (*a*) and self-similar temperature profiles across this layer (*b*).
Calculated data were obtained for different Grashof numbers Gr (10^6): 0.89 (*1*), 1.80 (*2*), 3.50 (*3*), 5.80 (*4*)

Fig. 5, *a* shows the dependence of the maximum values of the longitudinal velocity u^* on the coordinate x^* for different Grashof numbers. Each of these numbers corresponds to a range of x^* values where the change in the maximum longitudinal velocity linearly depends on the longitudinal coordinate x^*. An increase in the Grashof number leads to an increase in the maximum velocities, as well as to an increase in their growth rate.

The family of θ temperature profiles shown in Fig. 4, *a* can be described using the self-similar variable from [4], defined by the relation

$$\eta = y^* x^{*-2/5} \mathrm{Gr}^{1/5} \qquad (2)$$

Fig. 5, *b* shows the processed initial θ temperature profiles for different Grashof numbers. The values for the Grashof number $\mathrm{Gr} = 4.8 \cdot 10^6$, found experimentally in our study, are plotted in the figure. Additionally, the data from [5] are given for comparison.

The thickness of the near-wall region, i.e., how far along the normal to the disk the effect of the heated surface persists, should be found to better describe this region. Not only the dynamic thickness δ_u but also the thermal thickness δ_T is typically considered in case of non-isothermal flows because their values may differ. The thickness δ_T can be determined by choosing the minimum temperature value below which the heated surface has no effect. Using the dimensionless ratio for temperature and taking layer thickness, equal to 5% of the maximum dimensionless temperature, as the value sought for, the condition (criterion) for determining δ_T can be written as:

$$\delta_T = y^*|_{\theta=0.05}.$$

Other studies sometimes use different criteria. For example, an integral variant is proposed in [4]:

$$\delta_T = \int_0^\infty \theta dy^*.$$

Finding the dynamic thickness u of the near-surface natural convective layer seems to be a more difficult task, since the longitudinal (radial) velocity can take completely different values with distance from the disk surface, depending on the amount of air ejected into the near-surface layer. Some studies (see, for

example, [4]) propose using the following integral relation to find the dynamic thickness:

$$\delta_u = \int_0^\infty u^{*2}\, dy^*.$$

In our study, we have determined the dynamic thickness in view of the specifics of the dynamic near-surface layer where the shear stress generated as air moves along the fixed surface of the disk plays the primary role. In turn, friction is proportional to the derivative of the longitudinal velocity along the normal to the surface and decreases with distance from the disk. This means that this derivative can be used as a criterion for the boundary of the dynamic layer by choosing the appropriate limit value for this derivative, i.e.,

$$\delta_u = y^*\big|_{du^*/dy^*=e}$$

We have used the derivative value equal to 10 as the numerical criterion for e, i.e., e =10.

Notice that it is possible to further modify the variable y^* so that the values found for thermal and dynamic thickness coincide for different Grashof numbers. In our case, the temperature thicknesses shown in Fig. 5, *b* should be replaced with a single curve.

Fig. 6, *a* shows the dynamic and thermal thicknesses in terms of variables

$$(x^*;\ \delta_T \times \mathrm{Gr}^{1/5},\ \delta_u \times \mathrm{Gr}^{1/5}).$$

Notably, the dynamic layer substantially exceeds the thermal one in thickness and this difference markedly increases approaching the center of the disk.

Analysis of experimental and calculated data confirmed the well-known assumption that a thin layer of thermal conductivity exists in the near-wall region; convective heat transfer is practically absent in this layer, and its conductive heat transfer is characterized by a linear temperature profile [7]. The thickness δ_{CT} of this layer can be defined, for example, as the distance from the surface at which the temperature change differs from the linear distribution by 5%. The dependence of the thickness of the thermal conductivity layer on the longitudinal coordinate is also shown in Fig. 6, *a*.

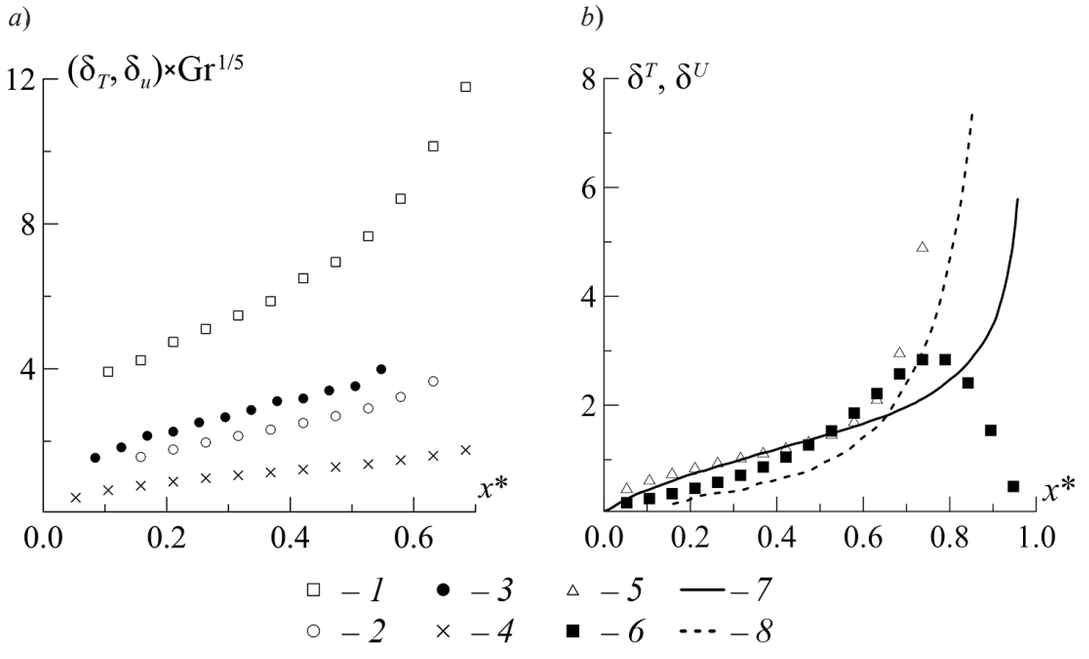

Fig. 6. Comparison of methods for determining the thermal thickness δ_T (*2*, *3*, *5* [4], *7* [4]) and dynamic thickness δ_u (1, 6 [4], 8 [4]) of the near-wall layer (in terms of modified variables) as a function of the longitudinal coordinate in this study (*a*) and in [4] (*b*) using experimental data (*3*, *5* [4], *6* [4]).
The figure shows the dependences as a function of x^* $\delta_u \times \mathrm{Gr}^{1/5}$ (*1*), $\delta_T \times \mathrm{Gr}^{1/5}$ (*2*), $\delta_T \times \mathrm{Gr}^{1/5}$ (*3*), $\delta_{CT} \times \mathrm{Gr}^{1/5}$ (*4*), $\delta_T^{\exp[4]}$ (*5*), $\delta_u^{\exp[4]}$ (*6*), $\delta_T^{[4]}$ (*7*), $\delta_u^{[4]}$ (*8*)

Fig. 6, *b* compares the thicknesses of the thermal and dynamic layers; the integral criteria proposed in [4] were used to find these quantities. Thermal thicknesses correlate well with each other, while dynamic thicknesses diverge significantly at $x^* \geq 0.7$. Our data indicate a decrease in dynamic thickness, which is quite natural, since the longitudinal (radial) component of the velocity vector tends to zero approaching the axis of the ascending plume. The reason for the dramatic increase in dynamic thickness obtained in [4] might be that an algorithm "combining" the solutions for the near-surface layer and the ascending plume was used in the calculations.

We should also note that a single criterion is insufficient to correctly determine the thicknesses of the dynamic and thermal layers, since the changes undergone by other parameters of the flow have to be taken into account. For example, the change in axial velocity has to be taken into account in choosing a criterion for determining the thickness of the dynamic layer, along with taking into account the nature of the changes in the longitudinal velocity at the boundary of the layer. Obviously, the role of axial velocity significantly grows approaching the region where the ascending jet evolves, and this factor should be taken into account along with the change in the longitudinal velocity.

In contrast to finding the thickness of the near-surface layer, finding its length is given much less attention in the literature, and in fact this problem is practically never discussed. Nevertheless, if the flow is regarded as a combination of a near-surface layer with an ascending flow, the boundaries of these regions in the longitudinal (radial) direction have to be determined, and this means that an appropriate criterion has to be chosen.

We propose to develop such a criterion based on a linear dependence of the maximum longitudinal velocity on the longitudinal coordinate (see Fig. 5, *c*).

Thus, the length of the near-surface layer depends on the value of the coordinate x^* for which the deviation of the curve of the maximum longitudinal velocity from the linear dependence is, for example, 1%. Then, for the case $\mathrm{Gr} = 3.5 \cdot 10^6$ (Fig. 7, *a*), the value $x^* = 0.62$ can be considered to be the boundary along the longitudinal coordinate of the near-surface layer.

This approach is of course justified not only by analysis of the longitudinal velocity component, but also by the corresponding dynamics of the changes in other parameters of the flow. Fig. 7,*b* shows the thermal and dynamic thicknesses of the near-surface layer. Evidently, the coordinate at which the thicknesses start to sharply increase corresponds well to the length of the near-surface layer. The change in the axial velocity (Fig 7,*c*), namely, a sharp increase, also occurs, starting from the value of the coordinate $x^*=0.62$.

It is convenient to analyze natural convective heat transfer of air with the heated hor-

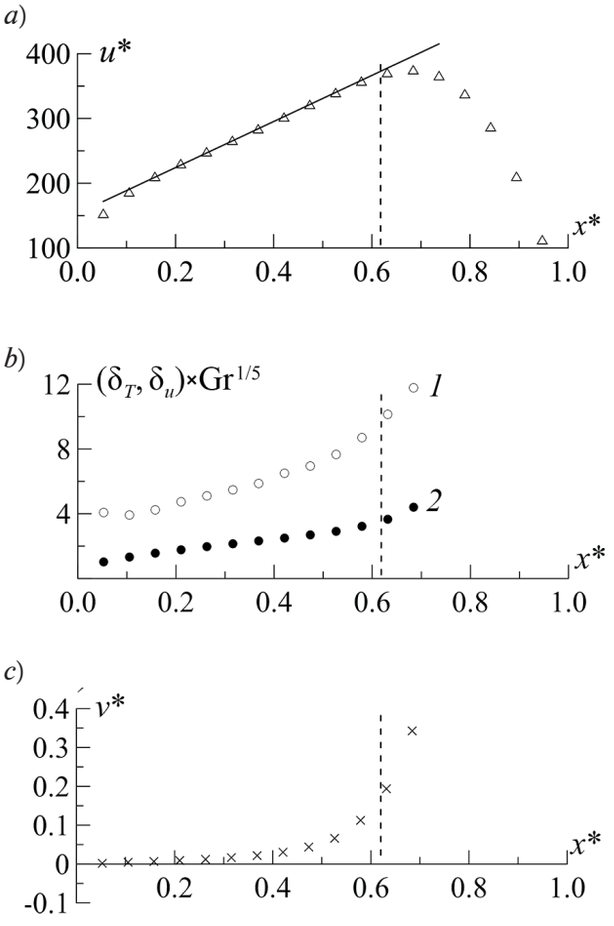

Fig. 7. Variation of calculated dimensionless characteristics of the near-wall layer over its entire length: maximum axial velocity (*a*), dynamic (*1*) and thermal (*2*) thickness (*b*), maximum axial velocity inside the layer (*c*)
Vertical dashes indicate the value $x^* = 0.62$ at which the curves deviate from linear dependences by 1%

izontal disk surface using the local Nusselt number, which is defined as follows:

$$\mathrm{Nu}_x = \frac{\alpha R\left(1-x^*\right)}{\lambda} = \frac{R(1-x^*)}{\left(T_a - T_w\right)}\left(\frac{\partial T}{\partial y}\right)\Bigg|_w, \quad (3)$$

where α is the heat transfer coefficient, determined from the assumption that a conductive heat transfer layer exists [6].

Fig. 8, *a* shows the change in the Nusselt number along the disk radius for a flow with the Gr = $5.4 \cdot 10^6$. The local Nusselt number takes the maximum value at the edge of the disk, and then monotonically decreases towards the center, which agrees well with our experimental data.

Fig. 8, *b* shows the distribution of the integral Nusselt number, found using the relation

$$\mathrm{Nu} = \frac{2\pi R^2}{S}\int_0^1 \mathrm{Nu}_{R(1-x^*)}(1-x^*)d(1-x^*),$$

depending on the Grashof number.

Such data are usually described by a power-law function which in case of laminar flow has the following form (see, for example, [7]):

$$\overline{\mathrm{Nu}} = C \cdot \mathrm{Gr}^{0.25},$$

where C is an empirical constant.

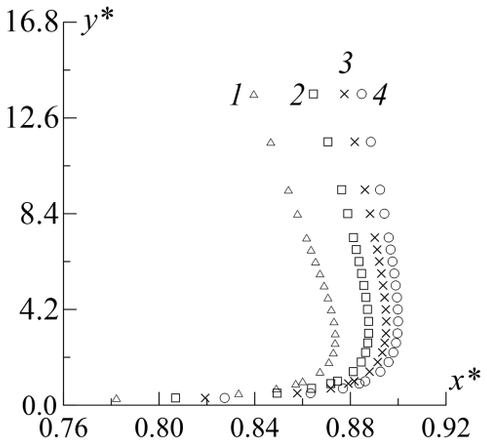

Fig. 9. Dimensionless thermal thickness of ascending plume for different Grashof numbers Gr (10^6): 0.89 (*1*), 1.8 (*2*), 3.5 (*3*), 5.8 (*4*)

The value of the constant C = 0.11 was taken in our study.

Let us consider the main patterns of the flow in the region of the ascending plume, for example, the geometric characteristics of the plume: temperature thickness or temperature radius b_T. The values of the coordinate $R - x$ for which the temperature is half its value on the axis can be taken as the temperature radius.

Fig. 9 shows the variation of the temperature radius of the plume for different Grashof numbers.

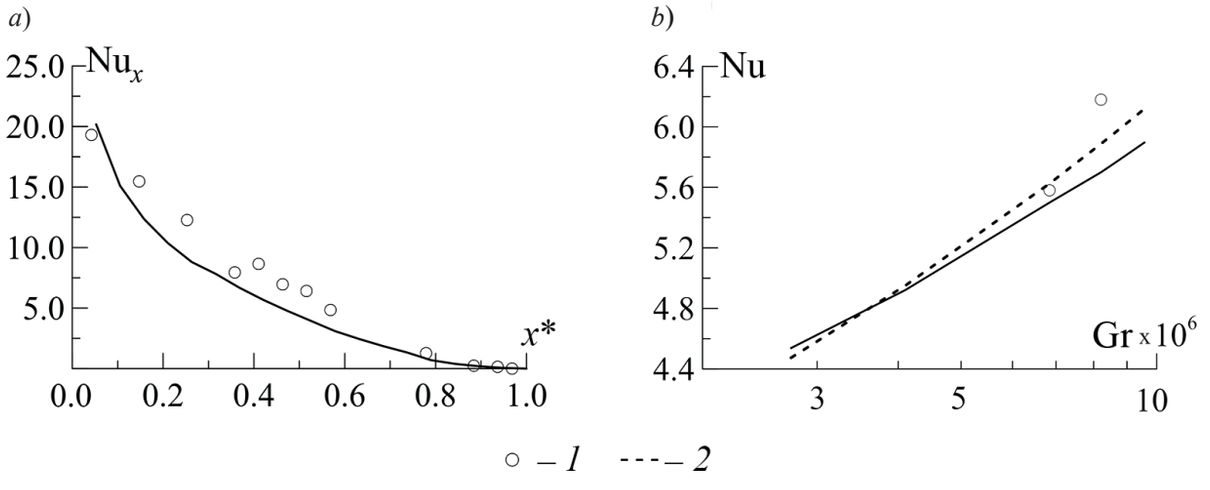

Fig. 8. Distributions of the local Nusselt number Nu_x over the radius of the disk with Gr = $5.4 \cdot 10^6$ (*a*) and the integral number Nu depending on the Grashof number (*b*). The distributions were obtained from the calculated (solid lines) and experimental (1) characteristics of heat transfer on the upper surface of the disk;
2 is the approximation of the experimental curve by the dependence $0.11 \cdot \mathrm{Gr}^{0.25}$ (Gr)

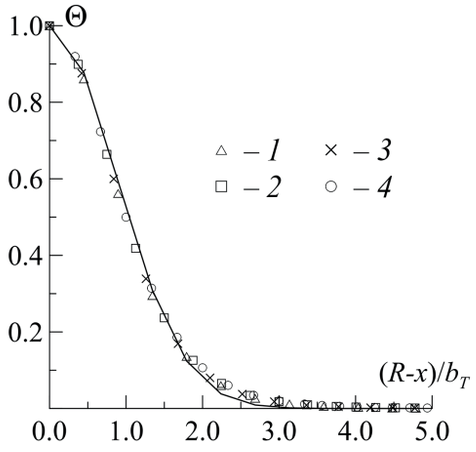

Fig. 10. Self-similarity of calculated temperature profiles in ascending flow at height $y^* = 8$ for different Grashof numbers Gr (10^6): 0.89 (*1*), 1.8 (*2*), 3.5 (*3*), 5.8 (*4*); solid line shows the approximating dependence

There is a segment where the plume narrows (the so-called "neck" [10]), after which the thickness monotonically increases with height. The position of the neck remains approximately the same with increasing Grashof numbers and the thickness of the plume decreases.

Several studies [1, 2, 8, 9] noted that the shape of the ascending plume was similar to jet flows, in particular, in temperature and velocity profiles. For example, the maximum temperature in a natural convective plume is observed on the flow axis, and then the temperature decreases monotonically. Additionally, temperature profiles of well-developed flow exhibit self-similarity in terms of variables $(R - x)/b_T$, θ, which is confirmed by the calculated data shown in Fig. 10.

Conclusion

We have reached the following conclusions based on the results of experimental and numerical simulation of a natural convection plume with small Grashof numbers.

The entire flow that is formed can be divided into two regions: the near-surface layer and the ascending flow.

Temperature and velocity profiles are self-similar in the well-developed sections of both regions.

Dynamic and thermal thicknesses of the near-surface layer were found by analysis of experimental data and the results of numerical simulation; criteria for determining these thicknesses were introduced. It was confirmed that the results of our analysis are in good agreement with the results obtained by other authors. We have proposed a criterion for determining the length of the near-surface layer based on analysis of the variation patterns of maximum longitudinal velocity in the layer. We have established that the length determined by this method does not contradict the physical dependences in the near-surface layer.

Even though the axial velocity component does not have a governing role in the near-surface layer, analysis of the behavior of this component was necessary both to construct a general model of the flow and to select many criteria, such as those determining the dynamic and thermal thicknesses, the length, etc.

We have obtained data on the heat transfer characteristics, namely, the distribution of the local Nusselt number over the surface of the disc, as well as the relationship between the integral Nusselt number and the Grashof number. The dependence we have found agrees well with the results obtained by other authors.

We have established that the temperature radius of the plume decreases with increasing Grashof numbers. The general patterns observed for the entire range of Grashof numbers are narrowing of the flow at a certain distance from the disk surface (the so-called "neck" region) and subsequent almost linear increase in the radius with increasing height.

Our findings indicate that steady near-wall flow which then becomes steady ascending flow can form despite the buoyancy force acting along the entire surface of the disk. A natural question to ask, then, is whether the given flow pattern persists with an increase in the intensity of disk heating. We have managed to uncover only several studies [8 – 10] hypothesizing that separation of the near-surface layer occurs at a sufficiently large distance from the center of the disk. Confirming this hypothesis can enhance our understanding of heat transfer over a heated horizontal disk.

The study was carried out with the financial support of the Russian Foundation for Basic Research as part of scientific project no. 18-31-00130.

REFERENCES

[1] **Y. Jaluria,** Natural convection: Heat and mass transfer, Pergamon Press, Oxford, 1980.

[2] **B. Gebhart, Y. Jaluria, R.L. Mahajan, B. Sammakia,** Buoyancy-induced flows and transport, Springer, 1988.

[3] **T. Fujii,** Theory of the steady laminar natural convection above a horizontal line source and a point heat source, Int. J. Heat Mass Transfer. 6 (7) (1963) 597–606.

[4] **J.H. Merkin,** Free convection above a uniformly heated horizontal circular disk, Int. J. Heat Mass Transfer. 28 (6) (1985) 1157–1163.

[5] **Md. Zakerullah, J.A.D. Ackroyd,** Laminar natural convection boundary layers on horizontal circular discs, J. Appl. Math. Phys. 30 (3) (1979) 427 –435.

[6] **W.W. Yousef, J.D. Tarasuk, W.J. McKeen,** Free convection heat transfer from upward-facing isothermal horizontal surfaces, J. Heat Transfer. 104 (3) (1982) 493–500.

[7] **E.F. Khrapunov, I.V. Potechin, Y.S. Chumakov,** Structure of a free convective flow over a horizontal heated surface under conditions of conjugate heat transfer, J. Phys.: Conference Series. 891 (December) (2017) 1–7.

[8] **Minh Vuong Pham, F. Plourde**, **Son Doan Kim,** Large-eddy simulation of a pure thermal plume under rotating conditions, Phys. Fluids. 18 (1) (2006) 015101.

[9] **F. Plourde, Minh Vuong Pham, Son Doan Kim, S. Balachandar,** Direct numerical simulations of a rapidly expanding thermal plume: Structure and entrainment interaction, J. Fluid Mech. 604 (2008) 99 –103.

[10] **J.M. Lopez, F. Marques,** Instability of plumes driven by localized heating, J. Fluid Mech., 736 (2013) 616 –640.

Received 03.09.2018, accepted 23.10.2018.

THE AUTHORS

KHRAPUNOV Evgenii F.
Peter the Great St. Petersburg Polytechnic University
29 Politechnicheskaya St., St. Petersburg, 195251, Russian Federation
hrapunov.evgenii@yandex.ru

CHUMAKOV Yuriy S.
Peter the Great St. Petersburg Polytechnic University
29 Politechnicheskaya St., St. Petersburg, 195251, Russian Federation
chymakov@yahoo.com

СПИСОК ЛИТЕРАТУРЫ

1. **Jaluria Y.** Natural convection: Heat and mass transfer. Oxford, GB: Pergamon Press, 1980. 326 p.

2. **Gebhart B., Jaluria Y., Mahajan R.L., Sammakia B.** Buoyancy-induced flows and transport. Springer, 1988. 1001 p.

3. **Fujii T.** Theory of the steady laminar natural convection above a horizontal line source and a point heat source // Int. J. Heat Mass Transfer. 1963. Vol. 6. No. 7. Pp. 597–606.

4. **Merkin J.H.** Free convection above a uniformly heated horizontal circular disk // Int. J. Heat Mass Transfer. 1985. Vol. 28. No. 6. Pp. 1157–1163.

5. **Zakerullah Md., Ackroyd J.A.D.** Laminar natural convection boundary layers on horizontal circular discs // J. Appl. Math. Phys. 1979. Vol. 30. No. 3. Pp. 427–435.

6. **Yousef W.W., Tarasuk J.D., McKeen W.J.** Free convection heat transfer from upward-facing isothermal horizontal surfaces // J. Heat Transfer. 1982. Vol. 104. No. 3. Pp. 493 –500.

7. **Khrapunov E.F., Potechin I.V., Chumakov Y.S.** Structure of a free convective flow over a horizontal heated surface under conditions of conjugate heat transfer//J. Phys.: Conference Series. 2017. Vol. 891. December. 7 p.

8. **Minh Vuong Pham, Plourde F., Son Doan Kim.** Large-eddy simulation of a pure thermal plume under rotating conditions // Phys. Fluids. 2006. Vol. 18. No. 1. P. 015101.

9. **Plourde F., Minh Vuong Pham, Son Doan Kim, Balachandar S.** Direct numerical simulations

of a rapidly expanding thermal plume: Structure and entrainment interaction // J. Fluid Mech. 2008. Vol. 604. Pp. 99–103.

10. **Lopez J.M., Marques F.** Instability of plumes driven by localized heating // J. Fluid Mech. 2013. Vol. 736. Pp. 616–640.

Статья поступила в редакцию 03.09.2018, принята к публикации 23.10.2018.

СВЕДЕНИЯ ОБ АВТОРАХ

ХРАПУНОВ Евгений Федорович – *аспирант Института прикладной математики и механики Санкт-Петербургского политехнического университета Петра Великого.*
195251, Российская Федерация, г. Санкт-Петербург, Политехническая ул., 29
hrapunov.evgenii@yandex.ru

ЧУМАКОВ Юрий Сергеевич – *доктор физико-математических наук, профессор Института прикладной математики и механики Санкт-Петербургского политехнического университета Петра Великого.*
195251, Российская Федерация, г. Санкт-Петербург, Политехническая ул., 29
chymakov@yahoo.com